Cell Reports

Article

Tryptophan-dependent and -independent secretions of tryptophanyl- tRNA synthetase mediate innate inflammatory responses

Graphical abstract

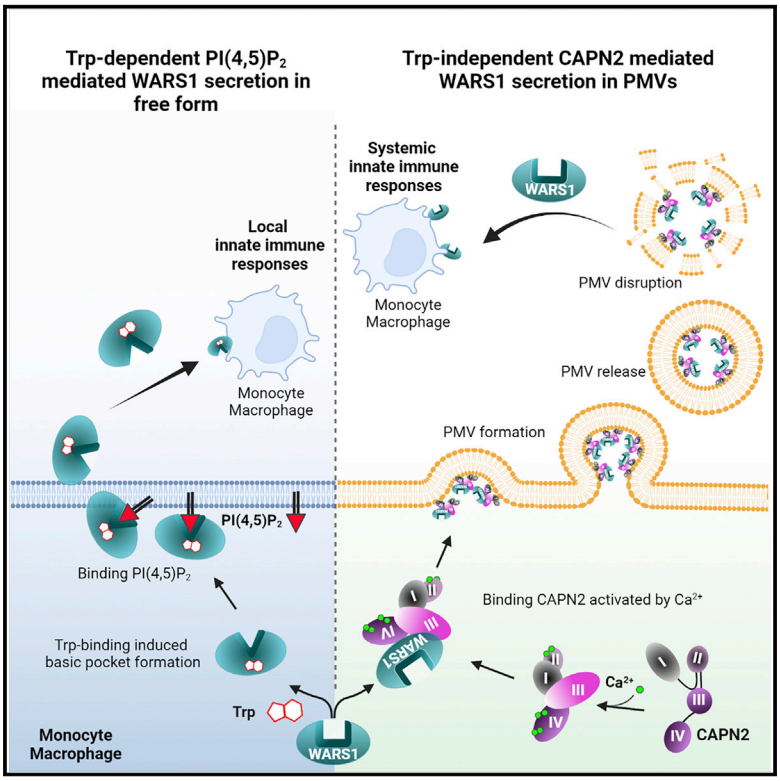

Authors

Tram Thuy Thuy Nguyen, Yun Hui Choi, Won-Kyu Lee, ..., Ji Hun Suh, Sunghoon Kim, Mirim Jin

Correspondence

mirimj@gachon.ac.kr

In brief

Tryptophanyl-tRNA synthetase 1 (WARS1) is an endogenous innate immune modulator secreted by monocytes/macrophages upon infection. In their study, Nguyen et al. elucidate the trafficking mechanisms that drive unconventional secretion of WARS1 and unravel the functions for tryptophan, $PI(4,5)P_2$, and calpain 2 in these processes.

Highlights

- WARS1 is secreted via two distinct pathways: free and plasma-membrane-derived vesicles (PMVs)
- Free WARS1 secretion depends on interactions with tryptophan and $PI(4,5)P_2$
- WARS1 secretion via PMVs is mediated by calpain 2 activated by calcium
- Both free and PMV-released WARS1 activate innate immune responses

Nguyen et al., 2023, Cell Reports *42*, 111905
January 31, 2023
https://doi.org/10.1016/j.celrep.2022.111905

CellPress

Cell Reports

CellPress
OPEN ACCESS

Article

Tryptophan-dependent and -independent secretions of tryptophanyl- tRNA synthetase mediate innate inflammatory responses

Tram Thuy Thuy Nguyen,[1] Yun Hui Choi,[2,3] Won-Kyu Lee,[4] Yeounjung Ji,[2,3] Eunho Chun,[1] Yi Hyo Kim,[1] Joo-Eun Lee,[5] Hyun Suk Jung,[5] Ji Hun Suh,[6] Sunghoon Kim,[6] and Mirim Jin[1,2,3,7,*]

[1]Department of Health Sciences and Technology, GAIHST, Gachon University, Incheon 21999, Korea
[2]Department of Microbiology, College of Medicine, Gachon University, Incheon 21999, Korea
[3]Lee Gil Ya Cancer and Diabetes Institute, Gachon University, Incheon 21999, Korea
[4]New Drug Development Center, Osong Medical Innovation Foundation, Cheongju 28160, Korea
[5]Department of Biochemistry, Kangwon National University, Chuncheon 24341, Korea
[6]Medicinal Bioconvergence Research Center, Institute for Artificial Intelligence and Biomedical Research, College of Pharmacy & College of Medicine, Gangnam Severance Hospital, Yonsei University, Incheon 21983, Korea
[7]Lead contact
*Correspondence: mirimj@gachon.ac.kr
https://doi.org/10.1016/j.celrep.2022.111905

SUMMARY

While cytoplasmic tryptophanyl-tRNA synthetase (WARS1) ligates tryptophan (Trp) to its cognate tRNAs for protein synthesis, it also plays a role as an innate immune activator in extracellular space. However, its secretion mechanism remains elusive. Here, we report that in response to stimuli, WARS1 can be secreted via two distinct pathways: via Trp-dependent secretion of naked protein and via Trp-independent plasma-membrane-derived vesicles (PMVs). In the direct pathway, Trp binding to WARS1 induces a "closed" conformation, generating a hydrophobic surface and basic pocket. The Trp-bound WARS1 then binds stable phosphatidylinositol (4,5)-biphosphate and inner plasma membrane leaflet, passing across the membrane. In the PMV-mediated secretion, WARS1 recruits calpain 2, which is activated by calcium. WARS1 released from PMVs induces inflammatory responses *in vivo*. These results provide insights into the secretion mechanisms of WARS1 and improve our understanding of how WARS1 is involved in the control of local and systemic inflammation upon infection.

INTRODUCTION

Aminoacyl-tRNA synthetases (ARSs) are a family of essential housekeeping enzymes that ligate amino acids to their cognate tRNA in protein synthesis.[1] Interestingly, many eukaryotic ARSs acquired additional biological functions beyond the classical catalytic activity during evolution and can be secreted into the extracellular space in response to diverse stresses to perform their biological functions.[1,2] For example, lysyl-tRNA synthetase (KARS1) is secreted from colorectal carcinoma cells via exosome to promote macrophage migration.[3] Glycyl-tRNA synthetase (GARS1) secreted by macrophages promotes apoptosis in cancer cells.[4] Human cytosolic tryptophanyl-tRNA synthetase (WARS1) is comprised of 417 amino acids, consisting of an N-terminal extension of 154 amino acids (N154), which has emerged in vertebrates, and a residual C-terminal domain.[5] The anti-codon domain (D354-A467) and catalytic domain (E82-S353) are embedded in the Rossmann dinucleotide-binding fold (RF) regions, where tryptophan (Trp) binds to Y159 and Q194 with a K_M of approximately 2 mM.[6] During protein synthesis, the recognition of Trp leads to a conformational change to generate a deep pocket for Trp binding, concomitant with the coupled movement of the N-terminal extension and the C-terminal domain, moving approximately 8 Å from an "open" to a "closed" conformation during amino acid activation.[7–9] On the contrary, this ancient protein has acquired noncanonical function as an innate immune activator. We reported that upon a variety of pathogenic infections, activated monocytes promptly release high levels of WARS1 prior to tumor necrosis factor α (TNF-α) production without *de novo* synthesis.[10,11] The secreted WARS1 binds to TLR4 and MD2 on macrophages via N154 (fully active domain for TLR4 activation) and induces neutrophil infiltration, concomitant with the production of proinflammatory cytokines and chemokines such as TNF-α, interleukin-6 (IL-6), IL-8, MIP-1α, and MCP-1 to expel invading pathogens.[10–12] Importantly, in the blood of patients with sepsis, a hyperinflammatory syndrome caused by severe infection, WARS1 secretion is dramatically increased, suggesting that it is not only a promising biomarker but also a therapeutic target, as massively secreted WARS1 can induce cytokine and chemokine storm.[10,13] Despite the important biological functions of extracellular WARS1, the mechanism underlying its secretion in monocytes remains unclear.

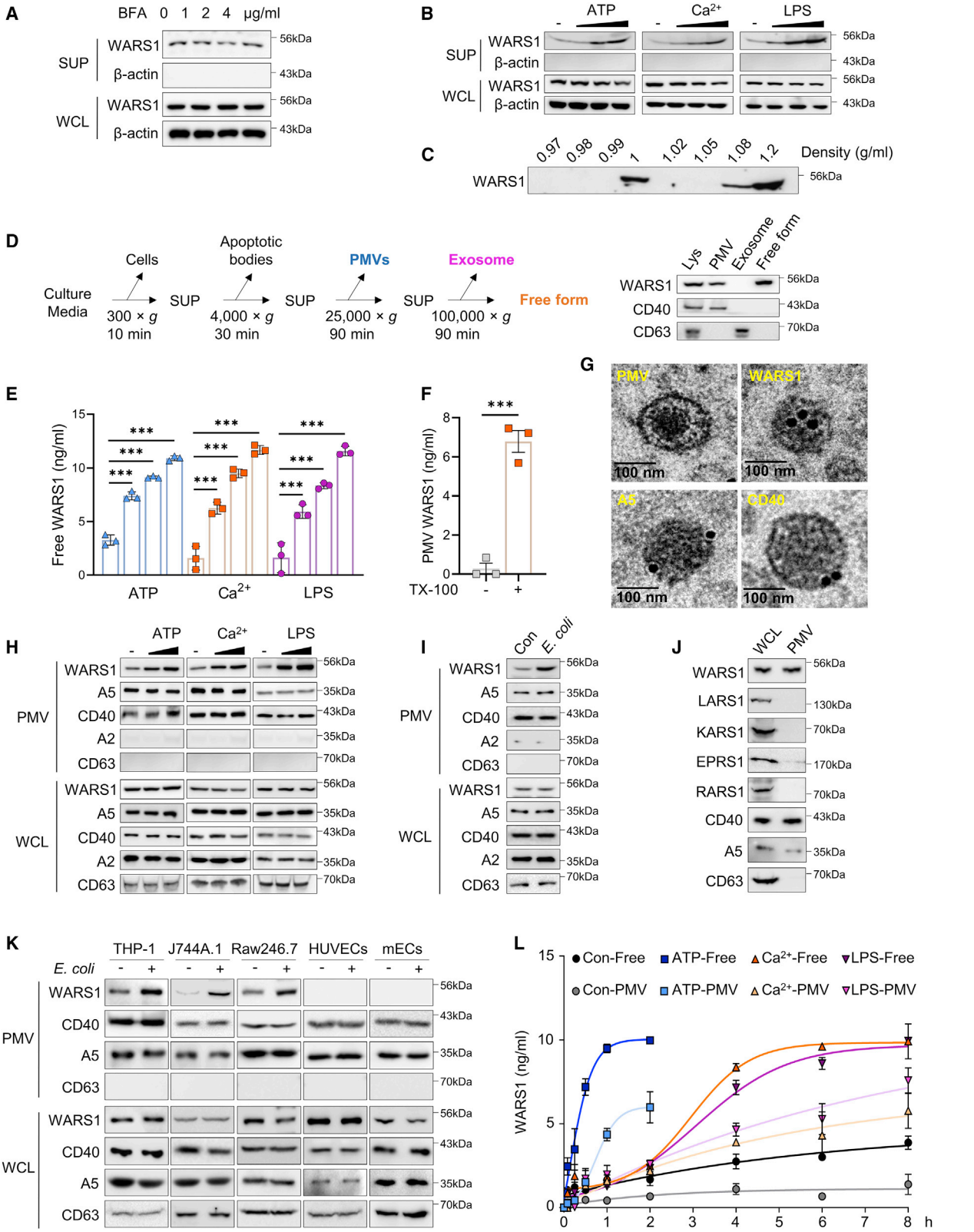

(legend on next page)

Proteins lacking a signal peptide utilize unconventional protein secretion (UPS) pathways that are not linked to the endoplasmic reticulum (ER) and Golgi transport.[14] Various kinds of UPSs have been described, including major pathways for distinct sets of cargoes that are secreted via membranes in the naked soluble form or that are associated with vesicles.[14–16] Various inflammatory stimuli trigger the translocation of leaderless proteins across the monocyte/macrophage plasma membrane via self-made lipidic pores, leading to the rapid and massive secretion of inflammatory proteins, including cytokines and chemokines.[15,17] Interactions with phosphatidylinositol (4,5)-biphosphate (PI(4,5)P_2), a lipid enriched in the inner leaflet of the plasma membrane, are necessary for membrane insertion, pore formation, and translocation.[16] Other proteins use membrane-bound organelles, such as exosomes and vesicles formed by late endolysosome/lysosome, for secretion.[14–17] Plasma-membrane-derived vesicles (PMVs), intact vesicles that bud from the cell surface and carry many proteins, have also been reported in monocytes/macrophages.[18] Interestingly, some proteins exit via multiple pathways. IL-1β, as a representative example, is secreted via membrane pores, membrane-bound lysosomes, and PMVs.[16,18]

We speculated that Trp contributes to the regulation of WARS1 secretion from monocytes based on several previous results: (1) some ARS functions are mediated and regulated by cognate amino acid binding,[1] (2) the activation of a Trp-selective transporter and Trp influx have been detected in activated monocytes/macrophages,[19] and (3) Trp binding changes the conformational structure of WARS1.[7–9] In this study, we show that increased concentrations of adenosine triphosphate (ATP), calcium (Ca^{2+}), and lipopolysaccharides (LPS) trigger monocytes to release WARS1 via two distinct pathways distinguished by Trp binding for innate inflammatory responses. The Trp-dependent form (free form) is mediated by PI(4,5)P_2, whereas the Trp-independent form (PMV form) is mediated by calpain 2 (CAPN2), a molecule involved in Ca^{2+}-activated and vesicle-associated protein secretion.[20]

RESULTS

WARS1 secretion via free form and PMVs in response to infectious stimuli in monocytes

WARS1 did not have any predicted signal peptides (as determined using the Signal IP database) and resided in the ER but not the Golgi (Figure S1A), and the secretion was not influenced by brefeldin A (BFA), an ER-Golgi transport inhibitor (Figure 1A). Accordingly, we speculated that WARS1 utilizes UPS pathways. To elucidate the mechanism underlying WARS1 secretion from monocytes, we treated cultured THP-1 cells, a human monocytic cell line, with various stimuli, including ATP, Ca^{2+}, and LPS, a bacterial cell wall component, as their levels are elevated at infection sites.[21–23] The concentration- and time-dependent secretion of WARS1 into the supernatant was determined by western blotting (Figures 1B and S1B). Secretion was initially detected 5 min to 4 h after treatment, and mRNA expression levels were not elevated until 12 h, indicating prompt secretion without *de novo* synthesis (Figures S1B and S1C). A density gradient analysis indicated that WARS1 was present in two fractions: ~1 g/mL and a density range of 1.08–1.2 g/mL (Figure 1C), suggesting that there were two different secreted forms. To further characterize these forms, the supernatant was fractionated according to the scheme shown in Figure 1D (left). Secreted WARS1 was present in the vesicle-free and PMV fractions, as determined by CD40,[24] but not in exosomes, as determined by CD63[14] (Figure 1D, right). WARS1, but not KARS1 or GARS1, is secreted in vesicles under physiological conditions

Figure 1. WARS1 secretion via free form and PMVs in response to infectious stimuli in monocytes

(A) Immunoblot analysis of WARS1 in THP-1 cell culture supernatants treated with BFA (6 h). The immunoblot figure represents three biologically independent experiments.

(B) Immunoblot analysis of WARS1 levels in THP-1 cell culture supernatants (SUPs) and whole-cell lysates (WCLs) in response to increasing concentrations of extracellular ATP (0–5 mM), Ca^{2+} (0–2.5 mM), or LPSs (0–10 μg/mL). The immunoblot figure represents three biologically independent experiments.

(C) Immunoblot analysis of WARS1 in the eight fractions of the 0.97–1.2 g/mL density ranges in THP-1 cell culture SUPs using sucrose gradient centrifugation. The immunoblot figure represents three biologically independent experiments.

(D) Schematic diagram displaying THP-1 cell culture SUP fractionation for free form and vesicle isolation (left panel). The presence of proteins in corresponding fractions was immunoblotted with the specific antibodies (right panel). The immunoblot figure represents three biologically independent experiments.

(E) WARS1 levels in free form determined by ELISA in THP-1 cell culture SUPs treated with increasing concentrations of ATP (0–5 mM), Ca^{2+} (0–2.5 mM), or LPS (0–10 μg/mL) (n = 3 biologically independent samples).

(F) WARS1 levels determined by ELISA in isolated PMVs from THP-1 cell culture SUPs untreated or treated with 0.1% Triton-X100 (TX-100), (n = 3 biologically independent samples).

(G) Immunogold staining of PMVs with specific antibodies for WARS1, A5, and CD40, known membrane-bound markers of PMVs. Scale bar: 100 nm. The figure represents three biologically independent experiments.

(H) Immunoblot analysis of proteins in isolated PMVs from THP-1 cell culture SUPs and WCLs treated with increasing concentrations of ATP (0–5 mM), Ca^{2+} (0–2.5 mM), or LPSs (0–10 μg/mL). The immunoblot figure represents three biologically independent experiments.

(I) Immunoblot analysis of proteins in isolated PMVs from human PBMC culture SUPs infected with K12 *E. coli* (MOI = 1) for 6 h. The immunoblot figure represents three biologically independent experiments.

(J) Immunoblot analysis of various ARSs present in WCLs and PMVs isolated from THP-1 cell SUPs. The immunoblot figure represents three biologically independent experiments.

(K) Immunoblot analysis of proteins in WCLs and isolated PMVs from various cell culture SUPs infected with K12 *E. coli* (MOI = 1) for 6 h. The immunoblot figure represents three biologically independent experiments.

(L) Time course of WARS1 secretion in both free form and PMVs from THP-1 cell culture SUPs stimulated with ATP, Ca^{2+}, or LPS. The WARS1 levels in SUPs and isolated PMVs after 0.1% TX-100 treatment were determined by ELISA (n = 3 biologically independent samples).

Data in (E) and (F) were analyzed using unpaired two-tailed Student's t test. Error bars indicate ±SD. ***$p < 0.001$.

See also Figure S1.

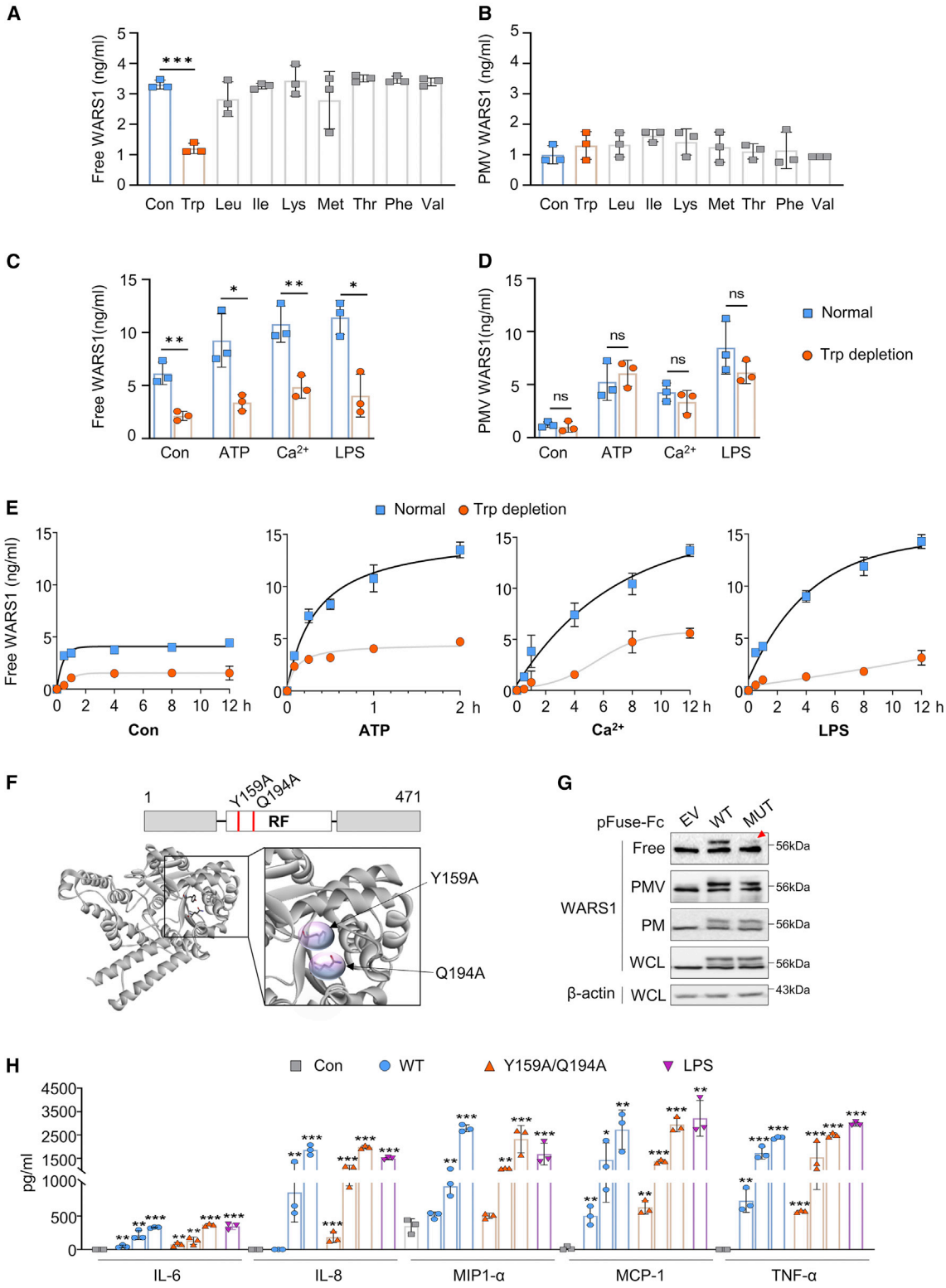

Figure 2. Blockade of Trp binding of WARS1 inhibits free-form secretion but not PMVs

(A and B) WARS1 levels in free (A) and PMVs (B) determined by ELISA from THP-1 cell culture SUPs after depletion of the indicated amino acids for 6 h (n = 3 biologically independent samples).

(legend continued on next page)

(Figure S1D).[3,4] Furthermore, upon exposure to infectious and inflammatory stimuli, we detected high levels of free WARS1 by ELISA, and the level of secretion was dose dependent (Figure 1E). For the vesicle form, WARS1 levels were determined from isolated PMVs following treatment with Triton X-100, a detergent for membrane lysis. Approximately 0.7 μg WARS1 was present in 10 μg PMVs from each unstimulated monocyte culture supernatant (Figure 1F). Consistent with these findings, electron microscopy indicated that WARS1 was present in the lumen of PMVs with annexin V (A5) and CD40 markers on their surfaces (Figure 1G). Increased levels of WARS1 were also determined following ATP, Ca^{2+}, and LPS treatment in the isolated PMV fractions, characterized by A5 and CD40 expression but not A2 and CD63, well-known exosome markers (Figure 1H).[14,24] Furthermore, in human peripheral blood mononuclear cells (PBMCs), K12 *E. coli* infection induced more abundant WARS1-loaded PMVs compared with levels in uninfected cells (Figure 1I). Other ARSs were not detected in the secretory microvesicles, including leucyl-tRNA synthetase (LARS1), lysine-tRNA synthetase (KARS1), glutamyl-prolyl-tRNA synthetase (EPRS1), and arginine-tRNA synthetase (RARS1) (Figure 1J). Increased WARS1 levels in PMVs caused by *E. coli* infection were observed in various human and murine monocytes/macrophages but not in endothelial cells, indicating monocyte/macrophage-specific secretion (Figure 1K). Finally, we examined the kinetics of WARS1 secretion in both the free and vesicle forms. WARS1 levels were higher in the vesicle-free fraction for all stimuli (Figure 1L). In particular, ATP promptly induced a substantial increase in free WARS1 as early as 5 min, while WARS1 loaded into secreted PMVs was detected at a later time. WARS1 secretion was not due to cell lysis, as the WST-1 assay showed no cell toxicity during the investigated time period except in response to ATP at >4 h, as reported previously[25] (Figure S1E). Taken together, these data suggest that infectious stimuli promote WARS1 secretion in monocytes/macrophages in two forms: vesicle free and PMVs.

Trp-dependent and -independent secretion of WARS1

To understand the role of Trp in WARS1 secretion, we tested the effects of various amino acids, including Trp, in THP-1 cells. Interestingly, the depletion of Trp, but not other amino acids, resulted in a significant reduction in free WARS1 secretion (Figure 2A). In contrast, amino acid depletion had no effect on WARS1-loaded PMVs (Figure 2B). Trp depletion dramatically lowered free WARS1 secretion after exposure to ATP, Ca^{2+}, and LPS (Figure 2C); however, WARS1 levels in PMVs remained unchanged (Figure 2D). The effect of Trp starvation on free WARS1 secretion was observed at a very early stage and was maintained over the entire investigation period (Figure 2E).

To test the importance of Trp binding, we generated WARS1 with Y159A and Q194A mutations to disrupt the Trp-binding pocket[19] (Figure 2F). The mutant WARS1 moved to the plasma membrane and was secreted in PMVs, similar to wild-type (WT) WARS1. However, we did not detect this mutant in the free-form fraction of the supernatant (Figure 2G), indicating that Trp binding is critical for free WARS1 secretion but not for secretion via PMVs. Further, we tested whether WARS1 lacking Trp binding affected inflammatory activity (Figure S2). As shown in Figure 2H, the Trp-binding mutant WARS1 could induce cytokine and chemokine secretion, similar to WT WARS1. These data suggest that Trp binding is critical for free WARS1 secretion but not for its inflammatory activity.

Binding of WARS1 with PI(4,5)P_2 at cell membrane is required for free-form secretion but not PMVs

To gain further insight into mechanisms underlying WARS1 secretion, we performed an interactome analysis and assigned proteins to functional pathways using data from DAVID, GO, and BioCarta (Figure 3A; Table S1). In addition to signaling pathways involved in protein synthesis and cell-cycle regulation, which are related to known WARS1 functions in the translation process,[5] phosphoinositides (PIPs) and the CAPN2 pathway, related to protein exocytosis and vesicle release, were overexpressed (Figure 3A). As depicted in Figure 3B, ATP, Ca^{2+}, and LPSs activate CAPN2 and G protein-coupled receptors (GPCRs), implicating PI(4,5)P_2 signaling in the regulation of exocytosis,[26] thus we then investigated the signaling pathways involved in WARS1 secretion. In human PBMC cultures, U73122 and Edelfosine, inhibitors of phospholipase C (PLC), leading to PI(4,5)P_2 accumulation by the inhibition of PI(4,5)P_2 cleavage into diacylglycerol (DAG) and 1,4,5-triphosphate (IP3), effectively boosted free WARS1 secretion to the same extent as the infectious stimuli, including ATP, Ca^{2+}, and LPSs (Figure 3C). There were no effects on TNF-α and IL-6 secretion at this early stage (Figure 3C). The PLC inhibitors dose-dependently induced free-form WARS1 secretion, with no effect on WARS1 levels in PMVs (Figures 3C, S3A, and S3B), implying that PI(4,5)P_2 contributes to free WARS1 secretion. Moreover, cAMP induction by the direct stimulation of adenylyl cyclases (ADCYs) with Forskolin had no influence (Figures 3C and S3C), and the ADCY inhibitor Ro20-1724 also showed no effect on WARS1 levels (Figures 3C and S3D). As the secretion of many

(C and D) WARS1 levels in free (C) and PMVs (D) from normal and Trp-depleted THP-1 cell culture SUPs treated with or without ATP, Ca^{2+}, or LPSs (n = 3 biologically independent samples).
(E) Time course of free-form WARS1 secretion in normal and Trp-depleted THP-1 cell culture SUPs treated with or without ATP, Ca^{2+}, or LPS (n = 3 biologically independent samples).
(F) Trp-binding double mutant (Y159A/Q194A) WARS1 (PDB: 1R6T).
(G) Immunoblot analysis of WARS1 in free, PMV, and plasma membrane (PM) fractions and WCLs in HEK293T cells transfected with the Trp-binding double-mutant plasmid for 72 h (◄, ectopic Trp binding mutant WARS1; EV, empty vector; WT, wild-type WARS1; MUT, Y159A/Q194A WARS1). The immunoblot figure represents three biologically independent experiments.
(H) Cytokine and chemokine levels in the PMA-differentiated THP-1 cells treated with PBS, WT WARS1 (25–100 nM), Y159A/Q194A WARS1 (25–100 nM), or LPS (10 ng/mL) for 8 h (n = 3 biologically independent samples).
Data in (A)–(D) and (H) were analyzed using unpaired two-tailed Student's t test. Error bars indicate ±SD. *p < 0.05; **p < 0.01; ***p < 0.001; ns, not significant. See also Figure S2.

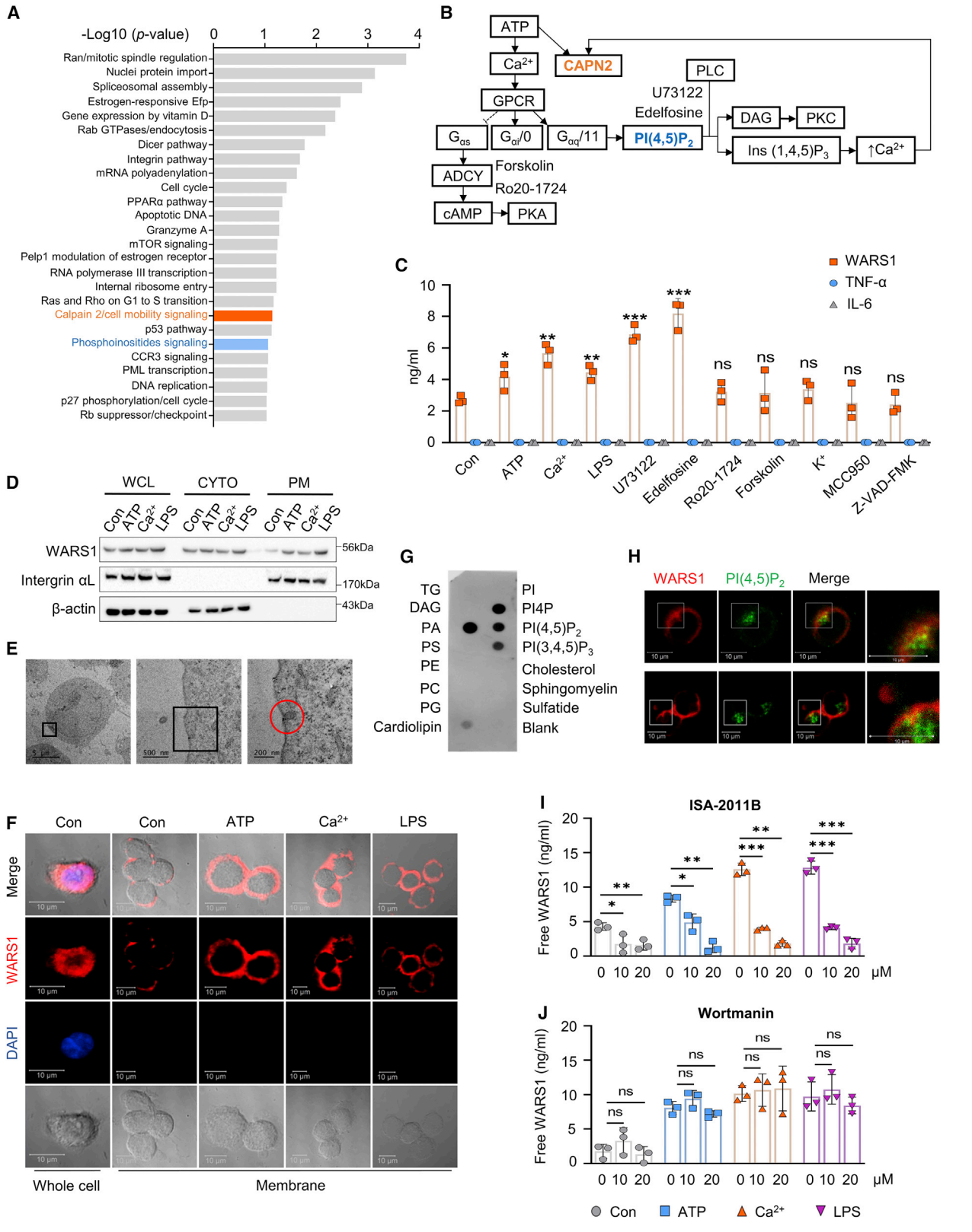

(legend on next page)

inflammatory proteins is mediated by the inflammasome and caspase activity,[27,28] we used K^+ influx or MCC950 to inhibit the inflammasome or Z-VAD-FMK for caspase inhibition. Neither inhibitor affected WARS1 secretion (Figures 3C and S3E–S3G), indicating no relevance of the inflammasome and caspase activity. As PIPs mediate protein exocytosis at the plasma membrane,[26] we examined the subcellular localization of WARS1 after ATP, Ca^{2+}, or LPS treatment. Compared with levels in the mock control, stimulated monocytes clearly expressed high levels of WARS1 on the membrane surface (Figure 3D). By electron microscopy, we detected WARS1 anchoring on the inner leaflet of the plasma membrane in monocytes (Figure 3E). Confocal microscopy confirmed that WARS1 was highly expressed on the plasma membrane of stimulated THP-1 cells (Figure 3F), implying a direct interaction of WARS1 with PI(4,5)P_2 at the membrane sites. By an *in vitro* lipid-overlay assay, we found that WARS1 directly bound to PIPs, including PI(4,5)P_2; phosphatidylinositol (3,4,5)-triphosphate (PI(3,4,5)P_3); phosphatidylinositol 4-phosphate (PI4P); and phosphatidic acid (PA), but not to other phospholipids (Figure 3G). Surface staining of monocytes showed high colocalization of WARS1 and PI(4,5)P_2 (Figure 3H). PI(4,5)P_2 and PI(3,4,5)P_3 play vital roles in protein exocytosis.[26,29] Treatment with the PI(4,5)P_2 inhibitor ISA-2011B significantly reduced free WARS1 secretion (Figure 3I) but not PMV-associated WARS1 release (Figure S3H). The PI(3,4,5)P_3 inhibitor Wortmannin had no effect on WARS1 secretion (Figures 3J and S3I). These data suggest that PI(4,5)P_2 binding is indispensable for free WARS1 secretion.

Trp binding of WARS1 generates a basic pocket for stable PI(4,5)P_2 binding for free-form secretion

To elucidate how secretion of the free form of WARS1 is governed by Trp and PI(4,5)P_2, we compared the binding affinities of WT and Trp-binding mutant WARS1 with PI(4,5)P_2. Mutant WARS1 clearly showed a weaker interaction with PI(4,5)P_2 than that of the WT (Figure 4A), suggesting that Trp binding promotes PI(4,5)P_2 interaction. A crystal structural analysis revealed that compared with the "open" conformational state unoccupied by Trp (Figures 4B and 4C, left, and S4A), Trp binding induced a "closed" conformational state, generating a hydrophobic region (Figure 4B, right) and a basic pocket (Figure 4C, right), where ionic interactions with the acidic phospholipid head of PI(4,5)P_2 are anticipated. Using *in silico* molecular docking, we selected putative critical residues in the basic pocket of WARS1 for PI(4,5)P_2 binding. WARS1 recombinant proteins carrying alanine mutations at residues N30, W88, V90, I98, Y100, E199, K200, K204, K277, K349, and S353 were generated and purified (Figure S4B) and tested for PI(4,5)P_2 binding affinity by ELISA. As shown in Figure 4D, E199, K200, K204, K277, and K349 mutants showed reduced signal intensities as compared to those for WT WARS1, confirming that these are PI(4,5)P_2 binding residues. K349 and K200, which were at opposite locations, played roles as a thumb and an index finger to capture the lipid head (Figure 4E). Indeed, a measurement of the length between K349 to K200 from the ζ nitrogen of the ammonia group at the terminal end of the atoms constituting the side chains of the two Lys revealed that the "closed" state with Trp had a much narrower distance compared with the "open" state (9.047 versus 14.675 Å, respectively), indicating a conformational change for stable interaction with PI(4,5)P_2 (Figure 4E). Based on these data, we built a model of the PI(4,5)P_2 bound in a pocket at the interface of WARS1 dimer (Figure S4C), with positive residues (E199, K200, K204, K277, and K349) having charged interactions with PI(4,5)P_2 (Figure S4D), with the mechanism governed by Trp binding, as illustrated in Figure S4E. Taken together, free WARS1 secretion occurs in a Trp- and PI(4,5)P_2-dependent manner by direct translocation across the membrane.

Binding of WARS1 with Ca^{2+}-activated CAPN2 is essential for PMV entry and secretion

Calpains are cytosolic proteases that are activated when intracellular Ca^{2+} increases or when cells are exposed to ATP and LPS; they are required for unconventional vesicle-mediated protein secretion in macrophages.[20,30,31] To clarify the WARS1 PMV secretion mechanism identified by the interactome analysis (Figure 3A), we purified the His-tagged calpain protein family, including CAPN1, CAPN2, and calpastatin, an endogenous inhibitor of calpain (Figure S5A), and performed an *in vitro* binding assay. As shown in Figure 5A, WARS1 bound directly to CAPN2, but not to CAPN1 or calpastatin, with a K_d value of 1.4 nM

Figure 3. WARS1 binds PI(4,5)P_2 at cell membrane for free-form secretion but not PMVs

(A) WARS1 interactome ontology classified using the functional annotation tool DAVID and results from GO term enrichment reflecting the highest p values from BioCarta pathways are shown.

(B) PI(4,5)P_2- and CAPN2-related signaling.

(C) WARS1, TNF-α, and IL-6 levels in human PBMC culture SUPs treated with the indicated stimuli for 2 h (n = 3 biologically independent samples).

(D) Immunoblot analysis of WARS1 in subcellular fractions from THP-1 cells treated with or without ATP, Ca^{2+}, or LPS. Cytoplasmic β-actin and PM integrin αL were detected to confirm the cytoplasm (CYTO) and PM fractions, respectively. The immunoblot figure represents three biologically independent experiments.

(E) Immunogold staining of WARS1 anchoring THP-1 inner leaflet PM. Scale bars: 5 μm, 500 nm, and 200 nm from left to right. The figure represents three biologically independent experiments.

(F) Immunofluorescence of WARS1 expression in THP-1 cells treated with the indicated stimuli. Scale bar: 10 μm. The figure represents three biologically independent experiments.

(G) Lipid-overlay assay. Immunodetection of His-tagged WARS1 binding to membrane-coated lipids using anti-His antibody. The figure represents three biologically independent experiments.

(H) Colocalization of WARS1 (red) and PI(4,5)P_2 (green) in THP-1 using immunofluorescence assay. Scale bar: 10 μm. The figure represents three biologically independent experiments.

(I and J) Free-form WARS1 levels from THP-1 cell culture SUPs treated with or without ATP, Ca^{2+}, or LPS in the presence of ISA-2011B (I) or Wortmannin (J) (n = 3 biologically independent samples).

Data in (C), (I), and (J) were analyzed using unpaired two-tailed Student's t test. Error bars indicate ±SD. *p < 0.05; **p < 0.01; ***p < 0.001; ns, not significant. See also Figure S3 and Table S1.

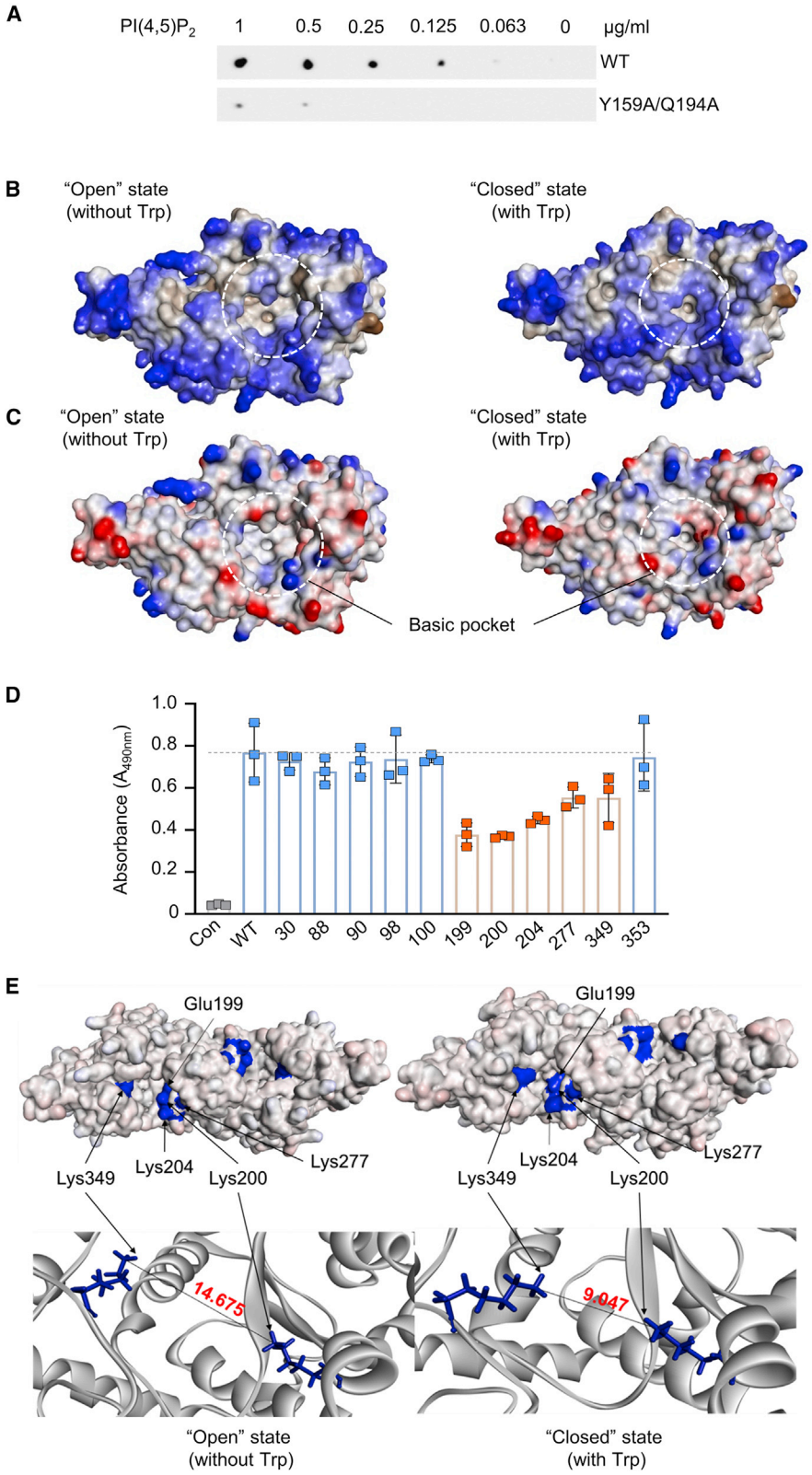

(legend on next page)

(Figure 5B). Monocytes electroporated with two small interfering RNAs (siRNAs) targeting CAPN2 abrogated WARS1 membrane expression (Figure 5C) and microvesicular WARS1 secretion in response to all stimuli (Figures 5C and 5D), indicating that WARS1 without CAPN2 was not anchored to the membrane and could not enter PMVs effectively. In contrast, the secretion of free WARS1 was not affected by CAPN2 silencing (Figure S5B). Treatment with MDL2817, a selective calpain inhibitor, yielded similar results. The inhibitor had no effect on free-form secretion (Figure S5C); however, it dose-dependently diminished the increase in vesicle-associated WARS1 secretion (Figure 5E). Immunoprecipitation assay showed that WARS1 bound CAPN2 in PMVs but not in free fractions, and their interaction increased by ATP, Ca^{2+}, or LPS stimulation (Figure S5D). To map the binding sites of WARS1 on CAPN2, an ELISA was carried out with a series of N-terminal WARS1 fragments (Figure S5E). All N-terminal fragments of WARS1 proteins showed no binding, indicating that the binding sites were in the C-terminal 154–471 aa of WARS1 (Figure 5F). Activated CAPN2 consists of four domains.[20] We found that D3 (356–511) and D4 (534–700) showed binding to WARS1, with D3 having stronger binding efficacy (Figures 5G and S5F). It is well known that Ca^{2+} activates calpain to promote conformational changes and cytoskeleton remodeling at the plasma membrane, thus facilitating the release of vesicles by cells.[20,30] Therefore, using EGTA, a Ca^{2+} chelator, we checked whether CAPN2-mediated WARS1 release is dependent on Ca^{2+} activity. As shown in Figure 5H, intracellular Ca^{2+} chelation abrogated the secretion of WARS1 in PMVs. In the case of calpain, dramatic structural changes after Ca^{2+} binding have been well described.[32] Therefore, we performed *in silico* docking experiments using CAPN2 with Ca^{2+} (PDB: 3BOW)[33] and Trp free WARS1 (PDB: 2QUK)[8] by Discovery studio 2021 software. Ca^{2+} binding induced conformation changes of CAPN2 (Figure S5G), favoring WARS1 dimer binding through D3 and D4, where D3 of CAPN2 is the center of WARS1 binding (Figure 5I, right). This model, which is consistent with the data from Figures 5F and 5G, had the highest stable energy status among 2,000 docked poses. On the contrary, the interaction of CAPN2 without Ca^{2+} and Trp free WARS1 was incapable of D3 binding but bound D2 instead (Figure 5I, left). Taken together, these data suggest that the secretion of WARS1 via PMVs depends on the interaction with CAPN2 activated by Ca^{2+}.

WARS1 release from PMVs activates innate inflammatory responses *in vivo*

To evaluate the functional significance of microvesicular WARS1, we collected PMVs from THP-1 cells electroporated with siNT control or WARS1-specific siRNA (siWARS1) (Figure S6A). When PMVs carrying WARS1 were used to treat differentiated macrophages, high levels of proinflammatory cytokines and chemokines, such as IL-6, MIP-1α, IL-8, MCP-1, and TNF-α, were produced; however, PMVs released from siWARS1-treated cells resulted in significantly reduced proinflammatory cytokine and chemokine activity (Figure 6A). To confirm these results *in vivo*, we created a mouse air pouch model and injected PMVs from either siNT or the two distinct sequences of siWARS1-treated cells, and LPS was used as a positive control (Figure 6B). Human WARS1 released from the PMVs was detected by western blotting in the air pouches, with a larger size than that of mouse WARS1, while no human WARS1 was detected in the phosphate-buffered saline (PBS)- or LPS-treated mice (Figure S6B). Furthermore, compared with the PBS-injected control group, siNT-PMV-injected mice had higher neutrophil and total cell counts, exceeding those for mice treated with LPS (Figures 6C and 6D). However, both siWARS1-PMV-injected groups showed significantly lower levels of neutrophil infiltration and total cell counts (Figures 6C and 6D). Highly increased levels of IL-6, MIP1-α, CXCL2, MCP-1, and TNF-α were detected in the air pouches of siNT-PMV- and LPS-treated groups (Figure 6E) compared with those in the naive control groups; however, all cytokine and chemokine levels were significantly lower in mice injected with both siWARS1-PMVs (Figure 6E). To confirm the presence of WARS1 in the free and PMV forms *in vivo*, we employed a cecal slurry (CS) sepsis mouse model. As shown in Figure 6F, peritoneal lavage fluid (PLF) of CS-inoculated mice had much higher levels of WARS1 in both free and PMV fractions compared with those in naive mice. In summary, these data indicate that WARS1 released from PMVs could contribute to innate inflammatory responses *in vivo*.

DISCUSSION

Specific recognition by WARS1 of its substrate Trp is critical for maintaining fidelity in protein synthesis.[7–9] During the process, Trp-binding energies generate an "induced-fit" transition, coordinating the binding pocket with ATP- and inorganic pyrophosphate (PPi)-binding subsites.[8,9,34] Interestingly, this characteristic has been adopted as secretion mechanism. In the cytoplasm, it is likely that the two states of WARS1 (i.e., Trp-bound and unbound forms) coexist and prefer different secretion routes. The noncovalent link with Trp changes WARS1 from an "open" allosteric state to a "closed" structure, with an increase in the hydrophobic residues, concomitant with the enclosure of the basic binding pocket to facilitate and stabilize $PI(4,5)P_2$ entry. This "closed" status captures $PI(4,5)P_2$ by generating electrostatic bonding at E199, K200, K204, K277, and K349 of

Figure 4. Trp-induced $PI(4,5)P_2$ binding is essential for WARS1 free-form secretion but not PMVs

(A) Immunodetection of His-tagged WT or Trp binding mutant WARS1 to a membrane-coated $PI(4,5)P_2$ using anti-His antibody. The figure represents three biologically independent experiments.

(B and C) Surface of WARS1 dimer structure with or without Trp by hydrophobicity (B) and charge distribution (C). The basic pocket of $PI(4,5)P_2$ binding site is marked with a circle.

(D) Binding affinities of a series of His-tagged WARS1 mutants with $PI(4,5)P_2$ (n = 3 biologically independent samples).

(E) Distance from the ζ nitrogen of the ammonia group at the terminal end of the atoms constituting the side chains (blue color) of K349 to K200.

Error bars indicate ±SD.

See also Figure S4.

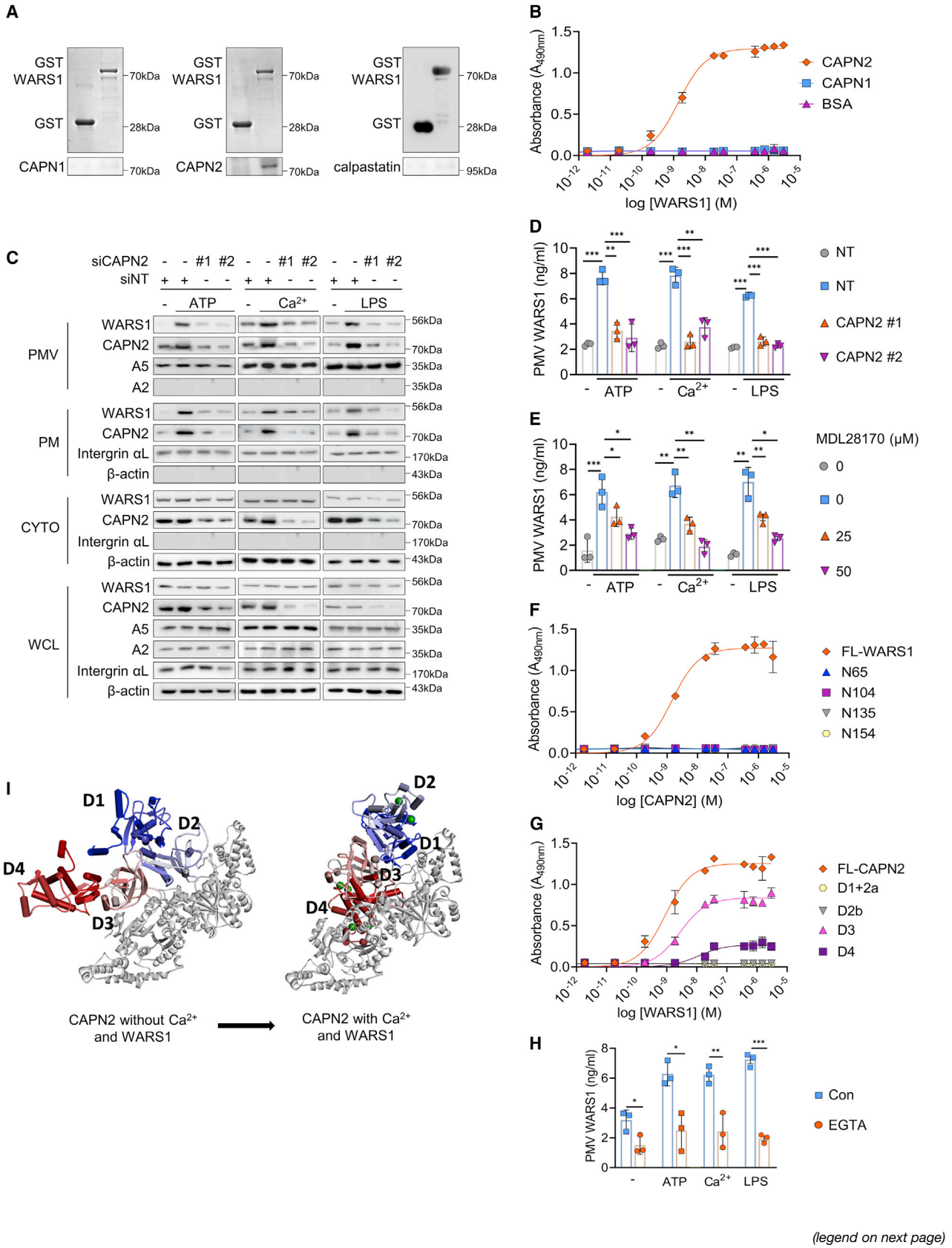

(legend on next page)

WARS1, resulting in recruitment to the inner leaflet and triggering release from the plasma membrane. Therefore, at a very early stage, infection-induced Trp influx may lead to massive free WARS1 translocation via the cell membrane into the extracellular fluid, enabling the prompt induction of inflammatory responses via TLR2 and/or TLR4 on proximal macrophages residing at local infection sites.[10–12] In other situations where the Trp reservoir is gradually reduced by infection-induced protein translation in monocytes, WARS1 without Trp binding in its "opened" state facilitates CAPN2-mediated PMV secretion. In infectious circumstances, intracellular Ca^{2+} is reported to be elevated in monocytes/macrophages, and binding with Ca^{2+} helps to lower the energy to activate CAPN2.[31,35,36] Activated CAPN2 is suggested to regulate the mobilization of vesicles to release sites and the molecular apparatus of vesicle trafficking.[20,30] Our data show that without CAPN2, WARS1 could not anchor the membrane leaflet and effectively enter the PMVs (Figure 5C). Binding of Ca^{2+} changes the CAPN2 structure, which makes D1 become more compact and D2a and D2b get closer and reinforces D3 and D4 of CAPN2 (Figure S5F). These structural changes facilitate D3 and D4 interaction with the C-terminal of WARS1, which is the most convincing model (Figure 5I). It seems that generation inside vesicles may help protect against overactive immune responses at proximal local sites by reducing naked WARS1 secretion. On the other hand, PMVs carrying WARS1 and a vast number of other inflammatory constituents, traveling over long distances, contribute to systemic inflammation, as observed in sepsis conditions.[37] Indeed, compared with quantities in healthy controls, increased PMVs have been reported in patients with sepsis and are associated with an increased severity of sepsis.[38,39] Consistent with these findings, plasma levels of WARS1 increase significantly as severity increases.[10,13] Thus, dual-secretion mechanisms enable WARS1 to initiate inflammation not only in its local environment but also far from its site of origin. Further, our data clarify how WARS1 residing in the lumen of these vesicles could exert extracellular functions. It has been suggested that PMVs (0.1–1 μm), which are larger than exosomes (30–100 nm), could be broken and thereby release their components or could be taken up by targeted cells.[40,41] In our study, the injection of PMVs isolated from THP-1 cells into air pouches of mice resulted in the release of human WARS1 (detected by a size difference compared with murine WARS1) (Figure S6B), supporting the former theory. In summary, our study provides insights on secretion mechanisms of WARS1, a host defense factor recruited from protein synthesis machinery and why N154, which is fully active as the TLR4-MD2 ligand, was attached to the catalytic domain of WARS1 during evolution. The answer may be that differentiation of secretion pathways through Trp fidelity in the catalytic domain can contribute to the control of extracellular activity, regulating innate immune responses at multiple levels including acute local reactions as well as systemic inflammatory response.

Limitations of the study

First, evidence on the translocation of free WARS1 via membrane pores was not provided. Second, although we identified the secreted PMVs based on their sizes (100–1000 nm in diameter) and surface biomarkers (A5, CD40) according to the methods accepted in this research field, their biogenesis (released from the plasma membrane through outward protrusion or budding) needs to be confirmed further. Third, as the crystal structure validation of WARS1-PI(4,5)P_2 and WARS1-CAPN2 interaction has not been provided, our data from *in silico* modeling support these interactions theoretically. Fourth, our proteomic analysis of WARS1's interactome revealed additional targets, such as proteins involved in the protein synthesis and cell-cycle regulation. Since we did not study these targets further, it remains unclear whether these proteins interact with WARS1 to modulate these processes.

STAR★METHODS

Detailed methods are provided in the online version of this paper and include the following:

- KEY RESOURCES TABLE
- RESOURCE AVAILABILITY
  - Lead contact
  - Materials availability
  - Data and code availability
- EXPERIMENTAL MODEL AND SUBJECT DETAILS
  - Cell culture
  - Animal models
- METHOD DETAILS

Figure 5. Binding of Ca^{2+}-activated CAPN2 is critical for WARS1 PMV secretion but not free form

(A) GST pull-down assay. GST or GST-tagged WARS1 binding with CAPN1, CAPN2, or calpastatin was determined by immunoblotting. The figure represents three biologically independent experiments.

(B) Binding affinities of WARS1 with CAPN1 and CAPN2 (n = 3 biologically independent samples).

(C) Immunoblot analysis of THP-1 cells electroporated with CAPN2 siRNAs and treated with indicated stimulus. Proteins present in PMV, PM, and CYTO fractions and WCLs were detected with the specific antibodies. The figure represents three biologically independent experiments.

(D) WARS1 levels of the PMV form in the SUPs of THP-1 cells electroporated with CAPN2 siRNAs and then treated with ATP, Ca^{2+}, or LPSs (n = 3 biologically independent samples).

(E) WARS1 levels of the PMV form in THP-1 cell culture SUPs treated with indicated stimulus in the presence of MDL28170 (n = 3 biologically independent samples).

(F) Binding affinities of various N-terminal WARS1 fragments with CAPN2 (n = 3 biologically independent samples).

(G) Binding affinities of various CAPN2 mutants with WARS1 (n = 3 biologically independent samples).

(H) WARS1 levels in PMVs of THP-1 cell culture SUPs treated with ATP, Ca^{2+}, or LPS in the presence of EGTA (n = 3 biologically independent samples).

(I) Ribbon drawing model of CAPN2 without Ca^{2+} or CAPN2 with Ca^{2+} (D3, D4) and WARS1 (C-terminal).

Data in (D), (E), and (H) were analyzed using unpaired two-tailed Student's t test. Error bars indicate ±SD. *$p < 0.05$; **$p < 0.01$; ***$p < 0.001$.

See also Figure S5.

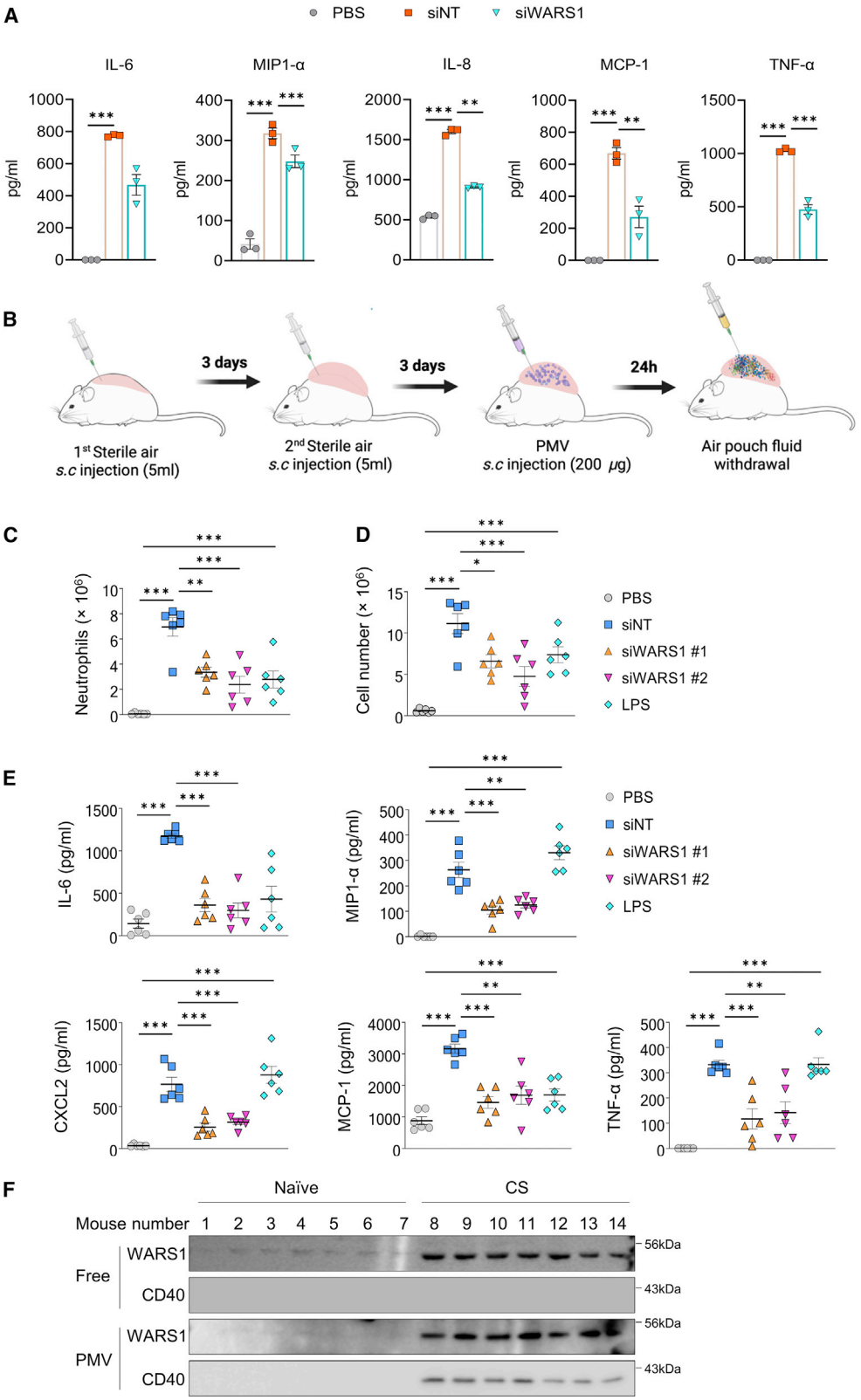

(legend on next page)

- *In silico* analysis
- Vesicle purification
- Immunogold-label EM
- Mass spectrometry
- Immunoprecipitation and western blot
- Subcellular fractionation
- Immunofluorescence
- Cytokine and chemokine detection
- Flow cytometry
- qPCR
- Recombinant protein purification

● QUANTIFICATION AND STATISTICAL ANALYSIS

SUPPLEMENTAL INFORMATION

Supplemental information can be found online at https://doi.org/10.1016/j.celrep.2022.111905.

ACKNOWLEDGMENTS

This research was supported by the Bio & Medical Technology Development Program of the National Research Foundation (NRF) of the Korean government (MSIT) (grant numbers NRF-2019M3E5D5064771 and NRF-2021R1A3B1076605); the Korea Health Technology R&D project through the Korea Health Industry Development Institute (KHIDI), funded by the Ministry of Health and Welfare; the Republic of Korea (grant number: HI20C0015); the Daegu-Gyongbuk/Osong Medical Cluster R&D project funded by the Ministry of Science and ICT; the Ministry of Trade, Industry and Energy; the Ministry of Health and Welfare, Republic of Korea (grant number: HI19C0763); and the Yonsei University Research Fund (grant number 2020-22-0356).

AUTHOR CONTRIBUTIONS

Conceptualization, T.T.T.N., Y.H.C., and M.J.; methodology, T.T.T.N., Y.J., E.C., Y.H.K., and J.-E.L.; software and formal analysis, T.T.T.N., Y.H.C., W.-K.L., H.S.J., and M.J.; writing – original draft, T.T.T.N.; writing – review & editing, S.K. and M.J.; supervision, M.J.

DECLARATION OF INTERESTS

M.J. is a founder and shareholder of MirimGENE.

Received: April 8, 2022
Revised: September 29, 2022
Accepted: December 9, 2022

REFERENCES

1. Yu, Y.C., Han, J.M., and Kim, S. (2021). Aminoacyl-tRNA synthetases and amino acid signaling. Biochim. Biophys. Acta Mol. Cell Res. *1868*, 118889. https://doi.org/10.1016/j.bbamcr.2020.118889.
2. Kwon, N.H., Fox, P.L., and Kim, S. (2019). Aminoacyl-tRNA synthetases as therapeutic targets. Nat. Rev. Drug Discov. *18*, 629–650. https://doi.org/10.1038/s41573-019-0026-3.
3. Kim, S.B., Kim, H.R., Park, M.C., Cho, S., Goughnour, P.C., Han, D., Yoon, I., Kim, Y., Kang, T., Song, E., et al. (2017). Caspase-8 controls the secretion of inflammatory lysyl-tRNA synthetase in exosomes from cancer cells. J. Cell Biol. *216*, 2201–2216. https://doi.org/10.1083/jcb.201605118.
4. Goughnour, P.C., Park, M.C., Kim, S.B., Jun, S., Yang, W.S., Chae, S., Cho, S., Song, C., Lee, J.H., Hyun, J.K., et al. (2020). Extracellular vesicles derived from macrophages display glycyl-tRNA synthetase 1 and exhibit anti-cancer activity. J. Extracell. Vesicles *10*, e12029. https://doi.org/10.1002/jev2.12029.
5. Jin, M. (2019). Unique roles of tryptophanyl-tRNA synthetase in immune control and its therapeutic implications. Exp. Mol. Med. *51*, 1–10. https://doi.org/10.1038/s12276-018-0196-9.
6. Ewalt, K.L., Yang, X.L., Otero, F.J., Liu, J., Slike, B., and Schimmel, P. (2005). Variant of human enzyme sequesters reactive intermediate. Biochemistry *44*, 4216–4221. https://doi.org/10.1021/bi048116l.
7. Pang, Y.L., Poruri, K., and Martinis, S.A. (2014). tRNA synthetase: tRNA aminoacylation and beyond. Wiley Interdiscip. Rev. *5*, 461–480. https://doi.org/10.1074/jbc.273.12.7052.
8. Shen, N., Zhou, M., Yang, B., Yu, Y., Dong, X., and Ding, J. (2008). Catalytic mechanism of the tryptophan activation reaction revealed by crystal structures of human tryptophanyl-tRNA synthetase in different enzymatic states. Nucleic Acids Res. *36*, 1288–1299. https://doi.org/10.1093/nar/gkm1153.
9. Ilyin, V.A., Temple, B., Hu, M., Li, G., Yin, Y., Vachette, P., and Carter, C.W., Jr. (2000). 2.9 A crystal structure of ligand-free tryptophanyl-tRNA synthetase: domain movements fragment the adenine nucleotide binding site. Protein Sci. *9*, 218–231. https://doi.org/10.1110/ps.9.2.218.
10. Ahn, Y.H., Park, S., Choi, J.J., Park, B.K., Rhee, K.H., Kang, E., Ahn, S., Lee, C.H., Lee, J.S., Inn, K.S., et al. (2016). Secreted tryptophanyl-tRNA synthetase as a primary defence system against infection. Nat. Microbiol. *2*, 16191. https://doi.org/10.1038/nmicrobiol.2016.191.
11. Lee, H.C., Lee, E.S., Uddin, M.B., Kim, T.H., Kim, J.H., Chathuranga, K., Chathuranga, W.A.G., Jin, M., Kim, S., Kim, C.J., and Lee, J.S. (2019). Tryptophanyl-tRNA synthetase stimulates innate immune responses against viral infection. J. Virol. *93*, e01291-18. https://doi.org/10.1128/JVI.01291-18.
12. Nguyen, T.T.T., Yoon, H.K., Kim, Y.T., Choi, Y.H., Lee, W.K., and Jin, M. (2020). Tryptophanyl-tRNA synthetase 1 signals activate TREM-1 via TLR2 and TLR4. Biomolecules *10*, 1283. https://doi.org/10.3390/biom10091283.
13. Choi, J.S., Yoon, B.R., Shin, J.H., Lee, S.H., Leem, A.Y., Park, M.S., Kim, Y.S., and Chung, K.S. (2020). Clinical value of full-length tryptophanyl-tRNA synthetase for sepsis detection in critically ill patients- a retrospective clinical assessment. Int. J. Infect. Dis. *97*, 260–266. https://doi.org/10.1016/j.ijid.2020.05.105.
14. Dimou, E., and Nickel, W. (2018). Unconventional mechanisms of eukaryotic protein secretion. Curr. Biol. *28*, 406–410. https://doi.org/10.1016/j.cub.2017.11.074.

Figure 6. WARS1 released from PMVs activates innate inflammatory responses *in vivo*

(A) Cytokine and chemokine levels in PMA-differentiated THP-1 cells treated with PBS or 100 μg PMVs collected from negative control siRNA (siNT) or WARS1 siRNA (siWARS1) electroporated-THP-1 cells (n = 3 biologically independent samples).

(B) Schematic diagram of mouse air pouch experiment

(C and D) Neutrophil numbers, identified by $CD11b^+$ and $Ly6G^+$ cells (C) and total cell numbers (D) collected from the air pouches (n = 6 mice per group).

(E) Cytokine and chemokine levels in exudates from the air pouches (n = 6 mice per group).

(F) Free and PMV WARS1 levels in PLF of naive or CS-inoculated mice detected by immunoblotting. Each lane represents the level of WARS1 in each mouse sample of each group (n = 7 mice per group).

Data in (A) and (C)–(E) were analyzed using unpaired two-tailed Student's t test. Error bars indicate ±SD. *p < 0.05; **p < 0.01; ***p < 0.001.

See also Figure S6.

15. Nickel, W., and Rabouille, C. (2009). Mechanisms of regulated unconventional protein secretion. Nat. Rev. Mol. Cell Biol. *10*, 148–155. https://doi.org/10.1038/nrm2617.

16. Rabouille, C. (2017). Pathway for unconventional protein secretion. Trends Cell Biol. *27*, 230–240. https://doi.org/10.1016/j.tcb.2016.11.007.

17. Stanley, A.C., and Lacy, P. (2010). Pathway for cytokine secretion. Physiology *25*, 218–229. https://doi.org/10.1152/physiol.00017.2010.

18. Théry, C., Ostrowski, M., and Segura, E. (2009). Membrane vesicles as conveyors of immune responses. Nat. Rev. Immunol. *9*, 581–593. https://doi.org/10.1038/nri2567.

19. Miyanokoshi, M., Yokosawa, T., and Wakasugi, K. (2018). Tryptophanyl-tRNA synthetase mediates high-affinity tryptophan uptake into human cells. J. Biol. Chem. *293*, 8428–8438. https://doi.org/10.1074/jbc.RA117.001247.

20. Khorchid, A., and Ikura, M. (2002). How calpain is activated by calcium. Nat. Struct. Biol. *9*, 239–241. https://doi.org/10.1038/nsb0402-239.

21. Rossol, M., Pierer, M., Raulien, N., Quandt, D., Meusch, U., Rothe, K., Schubert, K., Schöneberg, T., Schaefer, M., Krügel, U., et al. (2012). Extracellular Ca^{2+} is a danger signal activating the NLRP3 inflammasome through G protein-coupled calcium sensing receptors. Nat. Commun. *3*, 1329. https://doi.org/10.1038/ncomms2339.

22. Feske, S., Wulff, H., and Skolnik, E.Y. (2015). Ion channels in innate and adaptive immunity. Annu. Rev. Immunol. *33*, 291–353. https://doi.org/10.4049/jimmunol.174.11.7268.

23. Ojcius, D.M., Degani, H., Mispelter, J., and Dautry-Varsat, A. (1998). Enhancement of ATP levels and glucose metabolism during an infection by Chlamydia. J. Biol. Chem. *273*, 7052–7058. https://doi.org/10.1074/jbc.273.12.7052.

24. Eken, C., Gasser, O., Zenhaeusern, G., Oehri, I., Hess, C., and Schifferli, J.A. (2008). Polymorphonuclear neutrophil-derived ectosomes interfere with the maturation of monocyte-derived dendritic cells. J. Immunol. *180*, 817–824. https://doi.org/10.4049/jimmunol.180.2.817.

25. Mackenzie, A., Wilson, H.L., Kiss-Toth, E., Dower, S.K., North, R.A., and Surprenant, A. (2001). Rapid secretion of interleukin-1 beta by microvesicle shedding. Immunity *15*, 825–835. https://doi.org/10.1016/S1074-7613(01)00229-1.

26. Tan, X., Thapa, N., Choi, S., and Anderson, R.A. (2015). Emerging roles of PtdIns(4, 5)P_2-beyond the plasma membrane. J. Cell Sci. *128*, 4047–4056. https://doi.org/10.1242/jcs.175208.

27. Lu, B., Nakamura, T., Inouye, K., Li, J., Tang, Y., Lundbäck, P., Valdes-Ferrer, S.I., Olofsson, P.S., Kalb, T., Roth, J., et al. (2012). Novel role of PKR in inflammasome activation and HMGB1 release. Nature *488*, 670–674. https://doi.org/10.1038/nature11290.

28. He, Y., Hara, H., and Núñez, G. (2016). Mechanism and regulation of NLRP3 inflammasome activation. Trends Biochem. Sci. *41*, 1012–1021. https://doi.org/10.1016/j.tibs.2016.09.002.

29. Czech, M.P. (2000). PIP2 and PIP3: complex roles at the cell surface. Cell *100*, 603–606. https://doi.org/10.1016/S0092-8674(00)80696-0.

30. Välimäki, E., Cypryk, W., Virkanen, J., Nurmi, K., Turunen, P.M., Eklund, K.K., Åkerman, K.E., Nyman, T.A., and Matikainen, S. (2016). Calpain activity is essential for ATP-driven unconventional vesicle-mediated protein secretion and inflammasome activation in human macrophages. J. Immunol. *197*, 3315–3325. https://doi.org/10.4049/jimmunol.1501840.

31. Ji, J., Su, L., and Liu, Z. (2016). Critical role of calpain in inflammation. Biomed. Rep. *5*, 647–652. https://doi.org/10.3892/br.2016.785.

32. Moldoveanu, T., Hosfield, C.M., Lim, D., Elce, J.S., Jia, Z., and Davies, P.L. (2002). A Ca^{2+} switch aligns the active site of calpain. Cell *108*, 649–660. https://doi.org/10.1016/S0092-8674(02)00659-1.

33. Hanna, R.A., Campbell, R.L., and Davies, P.L. (2008). Calcium-bound structure of calpain and its mechanism of inhibition by calpastatin. Nature *456*, 409–412. https://doi.org/10.1038/nature07451.

34. Kapustina, M., and Carter, C.W. (2006). Computational studies of tryptophanyl-tRNA synthetase: activation of ATP by induced-fit. J. Mol. Biol. *362*, 1159–1180. https://doi.org/10.1016/j.jmb.2006.06.078.

35. Suzuki, K., Hata, S., Kawabata, Y., and Sorimachi, H. (2004). Structure, activation, and biology of calpain. Diabetes *53*, 12–18. https://doi.org/10.2337/diabetes.53.2007.S12.

36. Shao, H., Chou, J., Baty, C.J., Burke, N.A., Watkins, S.C., Stolz, D.B., and Wells, A. (2006). A spatial localization of m-calpain to the plasma membrane by phosphoinositide biphosphate binding during epidermal growth factor receptor-mediated activation. Mol. Cell Biol. *26*, 5481–5496. https://doi.org/10.1128/MCB.02243-05.

37. Robbins, P.D., and Morelli, A.E. (2014). Regulation of immune responses by extracellular vesicles. Nat. Rev. Immunol. *14*, 195–208. https://doi.org/10.1038/nri3622.

38. Monnamorn, L., Seree-Aphinan, C., Molika, P., Vichitkunakorn, P., Pattanapanyasat, K., Khwannimit, B., and Navakanitworakul, R. (2021). The concentration of large extracellular vesicles differentiates early septic shock from infection. Front. Med. *8*, 724371. https://doi.org/10.3389/fmed.2021.724371.

39. Raeven, P., Zipperle, J., and Drechsler, S. (2018). Extracellular vesicles as markers and mediators in sepsis. Theranostics *8*, 3348–3365. https://doi.org/10.3389/fcimb.2022.853840.

40. Bianco, F., Pravettoni, E., Colombo, A., Schenk, U., Möller, T., Matteoli, M., and Verderio, C. (2005). Astrocyte-derived ATP induces vesicle shedding and IL-1β release from microglia. J. Immunol. *174*, 7268–7277. https://doi.org/10.4049/jimmunol.174.11.7268.

41. Ratajczak, J., Wysoczynski, M., Hayek, F., Janowska-Wieczorek, A., and Ratajczak, M.Z. (2006). Membrane-derived microvesicles: important and appreciated mediators of cell-to-cell communication. Leukemia *20*, 1487–1495. https://doi.org/10.1038/sj.leu.2404296.

42. Starr, M.E., Steele, A.M., Saito, M., Hacker, B.J., Evers, B.M., and Saito, H. (2014). A new cecal slurry preparation protocol with improved long-term reproducibility for animal models of sepsis. PLoS One *9*, e115705. https://doi.org/10.1371/journal.pone.0115705.

STAR★METHODS

KEY RESOURCES TABLE

REAGENT or RESOURCE	SOURCE	IDENTIFIER
Antibodies		
Rabbit polyclonal anti-WARS1	Abfrontier	Cat#YF-PA15305
Mouse monoclonal anti-CAPN2 (clone E10)	Santa Cruz	Cat#sc-373966; RRID: AB_10917913
Mouse monoclonal anti-CAPN1 (clone D11)	Santa Cruz	Cat#sc-271313; RRID: AB_10610038
Mouse monoclonal anti-calpastatin (clone PI11)	Santa Cruz	Cat# sc-32324; RRID: AB_831042
Mouse monoclonal anti-β-actin (clone C4)	Santa Cruz	Cat#sc-47778 RRID: AB_626632
Mouse monoclonal anti-ANXA2 (clone C10)	Santa Cruz	Cat#sc-28385 RRID: AB_626677
Mouse monoclonal anti-Integrin αL (clone E1)	Santa Cruz	Cat#sc-374172 RRID: AB_10988435
Rabbit polyclonal anti-ANXA5	Abcam	Cat#ab14196 RRID: AB_300979
Rabbit monoclonal anti-CD40	Abcam	Cat#ab224639 RRID: AB_2883981
Mouse polyclonal anti-CD63	LifeSpan BioSciences	Cat#LS-C357785
Rabbit polyclonal anti-LARS1	LifeSpan BioSciences	Cat#LS-C290955
Mouse monoclonal anti-KARS1	Santa Cruz	Cat#sc-130405 RRID: AB_2196475
Rabbit polyclonal anti-EPRS1	Abcam	Cat#ab31531 RRID: AB_880047
Rabbit monoclonal anti-RARS1	Abcam	Cat#ab128956 RRID: AB_11145469
Rabbit polyclonal anti-GARS1	Abbexa	Cat#abx033785
Mouse monoclonal anti-CD11b-FITC (clone M1/70)	BD Biosciences	Cat#553310 RRID: AB_394774
Mouse monoclonal anti-Ly-6G-BV421 (clone 1A8)	BD Biosciences	Cat#562737 RRID: AB_2737756
Mouse monoclonal anti-GST (clone B14)	Santa Cruz	Cat#sc-138 RRID: AB_627677
Rabbit polyclonal Rhodamine (TRITC) IgG	Jackson ImmunoResearch	Cat#711-025-152 RRID: AB_2340588
Mouse polyclonal Fluorescein (FITC) IgG	Jackson ImmunoResearch	Cat#115-095-003 RRID: AB_2338589
Bacterial and virus strains		
E. coli DH5α	Dyne Bio	Cat#DYO1352
E. coli BL21-DE3	Dyne Bio	Cat#DYO1362
E. coli K12	ATCC	Cat#ATCC10798
Biological samples		
Clinical blood samples	Gachon University Gil Hospital	GCIRB2017-304
Chemicals, peptides, and recombinant proteins		
Adenosine 5'-triphosphate disodium salt hydrate (ATP)	Merck	Cat#A6419; CAS: 34369-07-8
Lipopolysaccharides (LPS) from *E. coli* O55:B5	Sigma-Aldrich	Cat#297-473-0;
Calcium chloride dehydrate ($CaCl_2$)	Sigma-Aldrich	Cat#223506; CAS: 10035-04-8

(*Continued on next page*)

Continued

REAGENT or RESOURCE	SOURCE	IDENTIFIER
Wortmannin	Sigma-Aldrich	Cat#W1628; CAS: 19545-26-7
CP-456773 sodium salt (MCC950)	Sigma-Aldrich	Cat#PZ0280; CAS: 256373-96-3
Z-VAD-FMK	Enzo Lifesciences	Cat#ALX-260-020; CAS: 220644-02-0
MDL-28170	Santa Cruz	Cat#sc-201301; CAS: 88191-84-8
ISA-2011B	MedChemExpress Lifesciences	Cat#HY-1693; CAS: 1184940-47-3
PI(4,5)P2 diC16	Echelon Biosciences	Cat#P-4516
PI(3,4,5)P3 diC16	Echelon Biosciences	Cat#P-3916
Triton X-100	Sigma-Aldrich	Cat#T9284; CAS: 1184940-47-3
NP-40	Sigma-Aldrich	Cat# 492016; CAS: 9016-45-9
Glycerol	Sigma-Aldrich	Cat#G5516; CAS: 56-81-5
Acetonitrile	Sigma-Aldrich	Cat#439134; CAS: 75-05-8
d-Desthiobiotin	Sigma-Aldrich	Cat#D1411; CAS: 533-48-2
Complete™ Protease Inhibitor Cocktail	Roche	Cat#11697498001
Gold nanoparticles	Sigma-Aldrich	Cat#741957
VECTASHIELD Antifade Mouting Medium with DAPI	Vector Laboratories Inc.	Cat#H-1200
Bovine Serum Albumin	Roche	Cat#10735078001; CAS: 75-05-8
Trichloroacetic acid solution	Sigma-Aldrich	Cat#T069
HEPES solution	Sigma-Aldrich	Cat#83264
Glutathione Sepharose High Performance GST-tagged protein purification resin	Cytiva	Cat#17527902
Mustang E Membane	Pall Corporation	Cat#17527902
Lipofectamine™2000 transfection reagent	Thermo-Fisher	Cat#11668019
Strep-Tactin Superflow column	Iba Lifesciences	Cat#2-1209-001
Critical commercial assays		
Membrane Lipid Strip	Echelon Biociences	Cat#P-6002
CellLight™ ER-GFP, BacMam 2.0	Thermo-Fisher	Cat#C10590
CellLight™ Golgi-GFP, BacMam 2.0	Thermo-Fisher	Cat#C10592
Plasma Membrane Protein Extration Kit	Abcam	Cat#ab65400
Neon™ Transfection System	Thermo-Fisher	Cat#MPK5000
Human IL-6 DuoSet ELISA	R&D Systems	Cat#DY206
Human IL-8 DuoSet ELISA	R&D Systems	Cat#DY208
Human MIP1-α DuoSet ELISA	R&D Systems	Cat#DY270
Human TNF-α DuoSet ELISA	R&D Systems	Cat#DY210
Mouse IL-6 DuoSet ELISA	R&D Systems	Cat#DY406
Mouse CXCL2 DuoSet ELISA	R&D Systems	Cat#DY452
Mouse MIP1- α DuoSet ELISA	R&D Systems	Cat#DY450
Mouse MCP-1 DuoSet ELISA	R&D Systems	Cat#DY479
Mouse TNF-α DuoSet ELISA	R&D Systems	Cat#DY410
Pierce LAL Chromogenic Endotoxin Quantitation Kit	Thermo-Fisher	Cat#88282

(*Continued on next page*)

Continued

REAGENT or RESOURCE	SOURCE	IDENTIFIER
Deposited data		
WARS1 interactome	This paper; PRIDE	Table S1; Accession number: PXD038250
Experimental models: Cell lines		
THP-1 cells	ATCC	Cat#TIB-202
J774.1 cells	ATCC	Cat#TIB-67
HUVECs cells	ATCC	Cat#PCS-100-010
Raw246.7 cells	ATCC	Cat#TIB-71
Mouse ECs	Cell Biologics	Cat#C57-6052
Experimental models: Organisms/strains		
Mouse: C57BL/6	DaehanBiolink Inc	N/A
Oligonucleotides		
		Table S2
Recombinant DNA		
Plasmid: pET28a	Sigma-Aldrich	Cat#69864
Plasmid: pGEX4T-1	Cytiva	Cat#GE28-9545-49
Plasmid: pFUSE-hIgG1-Fc2	InvivoGen	Cat#pfuse-hg1fc1
Plasmid: pEXPR-IBA105	IBA	Cat# 2-3505-000
Software and algorithms		
Discovery Studio 2021	Biovia	https://www.advanceduninstaller.com/BIOVIA-Discovery-Studio-2021-Client
GraphPad Prism	GraphPad Software	https://www.graphpad.com/scientificsoftware/prism/
Flowjo	BD Biociences	http://samtools.sourceforge.net/

RESOURCE AVAILABILITY

Lead contact

Further information and requests for resources and reagents should be directed to and will be fulfilled by the lead contact, Mirim Jin (mirimj@gachon.ac.kr)

Materials availability

This study did not generate new unique reagents.

Data and code availability

- Interactome data have been deposited at PRIDE and are publicly available as of the date of publication. Accession numbers are listed in the key resources table.
- This paper does not report any original code.
- Any additional information required to reanalyze the data reported in this paper is available from the lead contact upon request.

EXPERIMENTAL MODEL AND SUBJECT DETAILS

Cell culture

THP-1 (ATCC), J774.1 (ATCC), HUVECs (ATCC), Raw246.7 (ATCC) and mouse ECs (Cell Biologics) were maintained in Dulbecco's modified Eagle's medium (DMEM) supplemented with 10% FBS and 1% penicillin/streptomycin at 37^0C in a humidified incubator with 5% CO_2. Unless otherwise indicated, cells were stimulated with ATP (3 mM, for 15 min), $CaCl_2$ (1 mM, resulting in a total Ca^{2+} concentration of 1.42 mM, which is still in the physiological range,[21] for 4 h), and LPS (1 μg/mL, for 8 h). Transfection was performed using Lipofectamine 2000 (Invitrogen) for HEK293T cells, Neon transfection system (Invitrogen) for THP-1 cells.

For specific essential amino acid depletion, cells were cultured for 3 h with DMEM without L-Tryptophan (Trp), DMEM without L-Leucine (Leu), DMEM without L-Isoleucine (Ile), DMEM without L-Lysine (Lys), DMEM without L-Methionine (Met), DMEM without L-Threonine (Thr), DMEM without L-Phenylalanine (Phe), or DMEM without L-Valine (Val) were purchased from Welgene. Regular

DMEM supplemented with all amino acids was used as controls. All media were supplemented with 10% FBS and 1% penicillin/streptomycin.

Human peripheral blood mononuclear cells (PBMCs) were isolated from a cohort of 27 healthy male and female volunteers after approval by the Gachon University Bioethics Committee (IRB approval number GCIRB2017-304). Informed consent was obtained from the patients. Collected blood immediately was transferred to a Cell Preparation Tube (CPT, BD 362761, USA) and proceeded according to the manufacturer's protocol. PBMCs were resuspended with Roswell Park Memorial Institute (RPMI)-1640 medium (LM 011–01, Welgene, South Korea) supplemented with 2% Fetal Bovine Serum (FBS, Biowest) and 1% streptomycin/penicillin.

Animal models

Animal experiments complied with the guidelines of the Gachon University Animal Care and Use Committee (approval no. LCDI-2020-0088 and LCDI-2020-0089). C57BL/6 mice (male, 7 weeks old) were purchased from Daehan Biolink, Inc. (Chungbuk, Korea). Mice were adapted to the controlled conditions of 12:12h light/dark cycle, temperature of 22 ± 2°C, and humidity of 40–60%, with free access to standard food (LabDiet 5053, Orientbio) and sterilized water.

For the airpouch mouse model, mice were anesthetized, and subcutaneous dorsal pouches were created by injecting 5 mL of sterile air. Three days later, the pouches were reinjected with 5 mL of air. On day 6, 200 μg of PMVs was injected into the pouches. Control mice received sterile PBS. After 24 h, the animals were sacrificed and the pouches were washed with 3 mL of PBS containing 54 mM EDTA. The lavage fluid was immediately centrifuged at 4,000 *g* for 15 min at 4°C. The cells were analyzed by FACs, and the supernatants were divided for ELISA or for processing to separate vesicle fractions. Free fractions were used to detect WARS1 released from PMVs by western blotting.

For the CS sepsis mouse model, wild-type C57BL/6J mice were intraperitoneally (i.p.) inoculated with CS stock (20 mg per mouse). Mice were then sacrificed 12 h after inoculation for PLF collection by injecting 5 mL of PBS into the peritoneum of the mice, massaged for 2–3 min, and collected using a 5 mL-syringe. PLF was then fractionated into free and PMV fractions. CS stock was prepared by combining collected cecal contents, mixing with sterile water at a ratio of 0.5-mL of water to 100-mg of cecal content. The CS was then mixed with an equal volume of 30% glycerol in phosphate buffered saline (PBS), resulting in a final CS stock solution in 15% glycerol.[42]

METHOD DETAILS

In silico analysis

To compare conformational changes according to Trp amino acid binding, structural data of 2QUK (Trp-binding conformation) and 2QUH (Trp-unbinding conformation) in Protein Data Bank database (PDB) were used. To predict the binding site with $PI(4,5)P_2$ and effect of Trp in WARS1's conformation, two properties of the surface of the WARS1 structure, namely hydrophobicity and charge distribution, were calculated and observed. For $PI(4,5)P_2$ binding site prediction, the soluble site (inositol phosphate ring), with exception of the insoluble site (acyl chain) embedded in the lipid bilayer among $PI(4,5)P_2$, were used for docking analysis. For WARS1 (PDB: 2QUH) and CAPN2 (PDB : 1KFU and 2NQA) tertiary structure analysis, molecular docking and visualization, Discovery studio (version 2021, Biovia, USA) was used. Ranking of the poses was done by ZDOCK score. The 2,000 predicted docked conformations were subjected to refinement and re-ranking using the RDOCK module in order to remove clashes and optimize polar and charge interactions that helped to pick up a near-native conformation. The final-docked conformation was chosen from each docking process that had the best ZDOCK and RDOCK among all refined conformations.

Vesicle purification

PMVs were isolated by a modification of Eken et al. method.[24] Briefly, medium from cells were first centrifuged at 500 *g* for 5 min to remove cells. The supernatants were then centrifuged twice at 4,000 *g* for 30 min to remove cell debris and apoptotic bodies. The supernatant was sonicated in a sonicating water bath (Bioruptor, Diagenode) for 5 × 1 min to disperse aggregated exosomes. Supernatants were centrifuged at 25,000 *g* for 90 min to pellet PMVs. PMVs were then washed twice by resuspending in PBS. The protein concentration of isolated vesicles was measured and normalized using the BCA protein assay kit (Invitrogen). To compare relative levels in free and PMV fractions, 5 mL of cell supernatant was collected and fractionated into free and PMV fractions. PMV fractions were further lysed with 5 mL of 0.5% Triton X-100, and ELISA was performed using 100 μL of the free form or 100 μL lysed PMV fraction for WARS1 level detection and calculation.

Immunogold-label EM

THP-1 monocytes were fixed with 2.5% glutaraldehyde and 2% osmium tetroxide for 1 h at 4°C. They were then dehydrated with a graded acetone series and embedded into Spurr's medium (Electron Microscopy Sciences). The sections were made in 60-nm thickness horizontally to the plane of the samples using an ultramicrotome (RMCMTXL) and then mounted on nickel grids. Free aldehyde groups were quenched with 0.02 M glycine for 10 min. Sections were then rinsed in deionized water, floated for 1 h in PBS containing 1% BSA, and incubated directly in the primary antibody at 4°C for 1 h. Sections were rinsed several times with PBS-BSA (0.1% BSA in PBS) and floated for 1 h in IgG conjugated to 10-nm gold particles (Sigma-Aldrich) diluted 1:50 in PBS-BSA. The gold particle–labeled sections were counterstained with uranyl acetate and lead citrate. After the preparative steps of cryofixation,

the prepared sections were examined using a transmission electron microscope (H-7600; Hitachi) operating at 80 k and a JEM-1400 PLUS transmission electron microscope (JEOL).

Mass spectrometry

HEK293T cells transfected with pEXPR-IBA105 (empty vector) or Strep-tagged WARS1 were lysed in 120 mM Tris-HCl buffer (pH 8.0) containing 150 mM NaCl, 2 mM EDTA, 1% NP-40, 10% glycerol and protease inhibitor cocktail. The whole cell lysates were centrifuged at 16,000 *g* for 20 min at 4°C and protein mixtures containing Strep-tagged WARS1 were applied to a Strep-Tactin Superflow column (IBA) and washed with Strep wash buffer containing 100 mM HEPES (pH 8.0), 150 mM NaCl, and 1 mM EDTA. The column-bound proteins were eluted with a Strep elution buffer containing 100 mM HEPES (pH 8.0), 150 mM NaCl, 1 mM EDTA and 2.5 mM desthiobiotin. The eluted proteins were separated by SDS-PAGE and excised for in-gel digestion with trypsin. The digested peptides were subjected to mass analysis using an LTQ-Orbitrap Velos (Thermo Fisher Scientific) connected to an Easy-nano LC II system equipped with an autosampler. The peptide samples were then resuspended in 0.1% formic acid, and injected to reverse phase peptide trap EASY-Column and reverse phase analytical EASY-Column. Electrospray ionization (ESI) was performed using a 30 μm nanopore stainless steel online emitter (Thermo Fisher Scientific). The peptides were separated and eluted in a linear gradient of buffer B (0.1% formic acid in acetonitrile) over buffer A (0.1% formic acid in H_2O) from 10 to 40% at the flow rate of 300 mL/min. LTQ-Orbitrap Velos mass analyzer was used in positive ESI mode using collision-induced dissociation (CID) for peptide fragmentation. The obtained MS spectra were scanned from 350 to 2,000 m/z with a resolution of 100,000 and automatic gain control (AGC) target was set at 1,000,000 ions with a maximum fill time of 500 ms. A total of 20 data-dependent MS/MS scans were selected and fragmented in the ion trap with the isolation window of 2.0 m/z, AGC target value of 10,000 ions, normalized collision energy of 35, maximum fill time of 100 ms, and activation time of 10 ms. Dynamic exclusion was performed with repeat count of 1, exclusion duration of 180 s and dynamic exclusion list size of 500. The minimum MS ion count for triggering MS/MS was set at 5,000.

Immunoprecipitation and western blot

Cell lysates were subjected to SDS-PAGE and electro-transferred to a PVDF membrane. The membrane was blocked in Tris-buffered saline (TBS)-Tween (20 mM Tris-HCl [pH 7.6], 150 mM NaCl, and 0.25% Tween 20) containing 5% nonfat dry milk for 1 h, and then incubated with the indicated primary antibody overnight at 4°C. After washing three times with TBST, the membrane was stained with species-matched secondary antibodies (Cell Signaling). Blots were washed three times with TBST and imaged with the ImageQuant LAS-4000 system (GE Healthcare).

For WARS1 secretion, the culture media were collected and centrifuged at 500 *g* for 10 min. The supernatants were then centrifuged at 10,000 *g* for 30 min to remove membrane organelles, and precipitated with 12% TCA and incubated overnight at 4°C. Pellets were obtained by centrifugation at 17,000 *g* for 15 min and neutralized with 100 nM HEPES, pH 8.0. Proteins in the pellets were separated by SDS-PAGE and immunoblotted with an anti-WARS1 antibody.

WARS1 was cloned into pGEX4T-1 (GST-tag) vector. The recombinant proteins were overexpressed in *E. coli* BL21 strain. The bacterial cells were lysed by sonication three times (10 s duration with 50 s interval). GST-tagged WARS1 were purified by glutathione-sepharose high performance beads (GE Healthcare). Purified proteins were filtered using Mustang E. membrane (Pall Corporation). GST or GST-tagged-WARS1 in PBS was mixed with glutathione-sepharose beads at 4°C for 2 h. After 3 washings with PBS, recombinant CAPN1, CAPN2 or calpastatin proteins were added and the mixtures were incubated at 4°C for 4 h. Proteins binding to beads were subjected to western blot analysis.

Subcellular fractionation

THP-1 PM proteins were extracted using the plasma membrane protein extraction kit (Abcam, ab65400) according to the manufacturer's protocol.

Immunofluorescence

Cells were fixed in 4% paraformaldehyde with/without 0.1% Triton X-100 (permeabilized/non permeabilized condition). After 1 h blocking with 2% bovine serum albumin (BSA) at room temperature (RT), cells were stained with primary antibody for 1 h at RT. After three washes with PBS, cells were incubated with either tetramethyl rhodamine isothiocyanate (TRITC)-conjugated donkey anti-rabbit IgG or fluorescein isothiocyanate (FITC)-conjugated goat anti mouse IgG for 1 h at RT. Cells were counterstained with DAPI to label nuclei. After three washes with PBS, cells were analyzed using a Zeiss LSM 700 laser confocal microscopy system (Carl Zeiss, Inc., Thornwood, NY).

Cytokine and chemokine detection

The levels of TNF-α, MCP-1, MIP1-α, IL-6, IL-8 and CXCL2 in cell supernatants and airpouch lavage fluid were determined using commercially available ELISA kits according to the manufacturer's protocol. The levels of WARS1 in the cell supernatants were detected by a homemade ELISA kit according to the following protocols. Plates were coated with anti-WARS1 at 4°C for overnight and blocked at RT for 1 h; samples were incubated with detection antibody (Abfrontier, 1:500) and secondary antibody HRP-conjugated anti-rabbit IgG (Cell signaling, 1:3,000) at RT for 1 h. Next, 3,3′,5,5′-Tetramethylbenzidine (TMB) substrate (BD) was added and

incubated for 10 min at RT. The absorbance of samples was measured at 450 nm using a Versa Max microplate reader (Molecular devices) and analyzed using Soft max pro.[10]

Flow cytometry

Cells were stained with antibodies for 30 min on ice in a binding buffer (PBS with 0.5% BSA and 0.01% NaN_3) and analyzed on FACSCalibur (BD Biosciences) using FlowJo software (Flowjo LLC).

qPCR

qPCR was conducted using an iQ5 multicolor real-time PCR detection system (Bio-Rad). The primer used for human *WARS1* (Forward, 5'-AAG AAT TCA TGC CCA ACA GTG AGC CC-3'; Reverse, 5'-AAC TCG AGC TAC CCT GGA GGA CAG TCA GCC TT-3'), human *β-actin* (Forward, 5'- CAT GTA CGT TGC TAT CCA GGC-3'; Reverse, 5'-CTA CCT TAA TGT CAC GCA CGA T-3').

Recombinant protein purification

A series of human WT and mutant WARS1, CAPN1, CAPN2, and calpastatin were cloned into pET28a (His-tag) vector. The recombinant proteins were overexpressed in *E. coli* BL21 strain and endotoxin was removed using a Mustang E. membrane (Pall Laboratory, 17527902). Endotoxin levels were measured using the Pierce LAL Chromogenic Endotoxin Quantification Kit (88282; Thermo Fisher).[10]

QUANTIFICATION AND STATISTICAL ANALYSIS

All graphs shown in main and supplementary figures were plotted using Prism 8 (GraphPad). Data are presented as Mean ± Standard Deviation (SD) and n values in the graphs indicate number of samples used for quantification as mentioned in the figure legends. Significance values for each dataset were calculated using a two-tailed unpaired *t* test. Significance values are indicated as follows: ns, not significant; *, $p < 0.1$; **, $p < 0.01$; ***, $p < 0.001$.